Micro X-ray CT Imaging of Sediments under Confining Pressure

Mandy Schindler and Manika Prasad, Center for Rock Abuse, Colorado School of Mines*

SUMMARY

We developed a pressure and temperature control system for use inside the micro X-ray CT scanner Xradia 400. We succeeded in building a pressure vessel that can be pressurized to 34.5 MPa (5000 psi) while being transparent to X-rays. The setup can currently be cooled to -5°C and heated to 40°C. We were able to observe grain damage and porosity reduction due to applied confining pressure in clean quartz sand samples and quartz sand and bentonite samples. The pressure control system in combination with ultrasonic transducers will allow to visually observe pore scale changes in rock samples (such as crack closure, grain damage, porosity reduction, changes in saturation) while simultaneously identifying their influence on elastic properties.

INTRODUCTION

We are implementing a pressure and temperature control system for use inside the Xradia-400 μCT machine. Goal of this work is to be able to conduct μCT images of rock samples while pore and confining pressure is applied. The temperature control is mainly intended for scans of gas-hydrate bearing sediments. In addition to pressure and temperature control we plan to conduct ultrasonic P-wave velocities simultaneously with μCT imaging. The combination of imaging and velocity measurements will give us insight in pore-scale changes in the rock and their influence on elastic properties.

EXPERIMENTAL METHOD

The Xradia-400 micro X-ray CT works at a maximum source power of 10 W and source voltage of 150 keV. The maximum size of field of view is 2 by 2 inches (50.8 mm * 50.8 mm). The highest resolution is 1 m. For high resolution scans the field of view is significantly smaller (e.g. for a resolution of 1 μm the field of view is reduced to 1 mm by 1 mm) and for a big field of view the resolution is reduced (e.g. for maximum size of field of view, resolution is 70 μm). Thus, we used a medium resolution (5 μm) and medium size of field of view (5 mm * 5 mm).

Figure 5 shows a schematic of the experimental setup inside the μCT machine. Confining pressure is applied through an ISCO pump located outside of μCT machines lead enclosure. We use water as a confining fluid. Currently, the pressure cell is closed off with a valve and detached from the pump before the imaging process in order to avoid movement during the imaging.

For the temperature control system, air from a compressor is

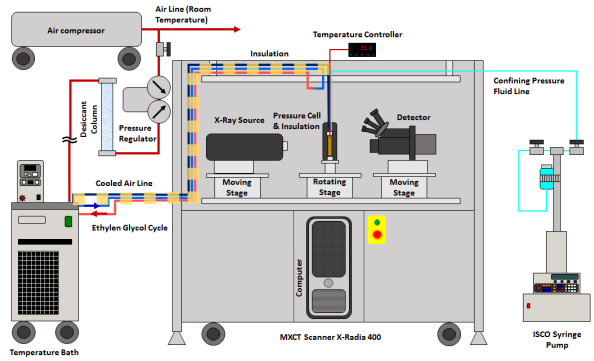

Figure 1: : Schematic of the μCT machine with pressure cell and temperature and pressure control systems

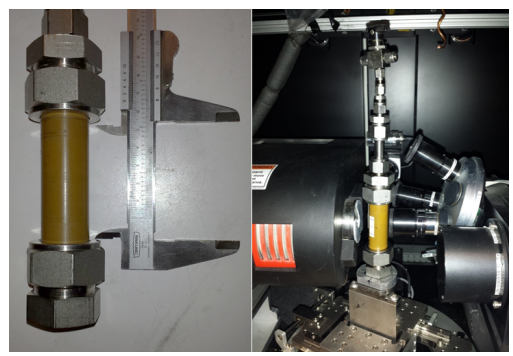

Figure 2: Torlon pressure cell with 25.4 mm outer diameter and 14 mm inner diameter

led through a copper coil in a temperature bath filled with ethylene glycol. The temperature bath can be regulated from -30°C to +70°C. The air is then used to cool or warm the sample inside the μCT scanner. The air hose is paired with a hose loop flowing ethylene glycol. Both hoses are insulated until they reach the sample. The pressure cell containing the sample is covered with a plastic cylinder to confine the temperated air to a small volume around the pressure cell.

We built two pressure cells consisting of Torlon tubing with stainless steel Swagelog fittings on both ends (Figures 2 and 3). The smaller cell has an outer diameter of 12.7 mm (0.5 inches) and an inner diameter of 8 mm; the bigger cell has an outer diameter of 25.4 mm (1 inch) and an inner diameter of 14 mm. The cells have been tested for pressures up to 34.5 MPa (5000 psi). We chose Torlon as material for the pressure cells since it proved to withstand high pressures while having a low density and thus being transparent to X-rays. Higher density materials, like stainless steel, would cause significant attenuation of X-rays and thus a much longer scanning time

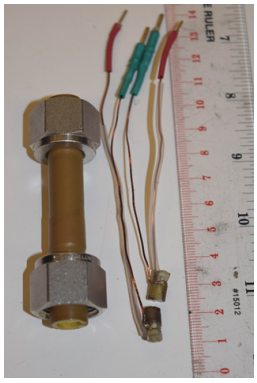

Figure 3: Torlon pressure cell with 12.7 mm outer diameter and 8 mm inner diameter along with P-wave ultrasonic transducers. The PZT crystals are 3 mm in diameter.

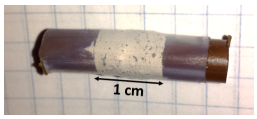

Figure 4: Sample of coarse-grained quartz sand with 30wt% bentonite between Torlon end pieces and heat-shrink jacket

and artefacts in the CT images.

We built ultrasonic transducers that fit into both pressure vessels (Figure 3). The transducers consist of piezoelectric PZT P-wave crystals and cylindrical pieces of Torlon. Both are connected with conductive epoxy. On the edges and the outward facing side of each PZT crystal (facing away from the sample) we applied a rounded layer of K20 epoxy to avoid the reflection of waves from this direction. The ground wires are attached to the Torlon buffer and the signal wire is attached to the PZT crystal. The PZT crystals are squares with the dimensions of 2.5 mm by 2.5 mm. This very small size was necessary to fit the transducers into the pressure vessel (inner diameter: 8 mm) while still being able to lead all four wires past the upper transducers. The small dimensions of the transducers led us to the decision to include only P-wave crystals and no S-wave crystals. The S-wave signal that could be acquired under the described conditions would not be suitable for interpretation. The ultrasonic transducers were not yet included in the pressure setup. Thus in this study, we will focus solely on the imaging part of the experiment.

The sample shown in Figure 4 consists of a 1-cm long sediment pack placed between two Torlon end pieces which will later be replaced by the ultrasonic transducers. The sample was jacketed with heat shrink tubing and clamped with steel wires on both ends. As sediment we used coarse grained quartz sand mixed with 30t% bentonite. The sample was dry; pore pressure was not applied.

We conducted 3 cycles of confining pressure increase to 13.8 MPa (2000 psi) and subsequent decrease to atmospheric pressure. The confining pressure was increased for 16 hours before imaging and decreased back to atmospheric pressure for 8 hours prior to imaging to allow the sample to equilibrate. Multiple pressure cycles were performed to observe if the changes to the sample are reversible and whether there are further changes in a pre-compacted sample when pressurized again.

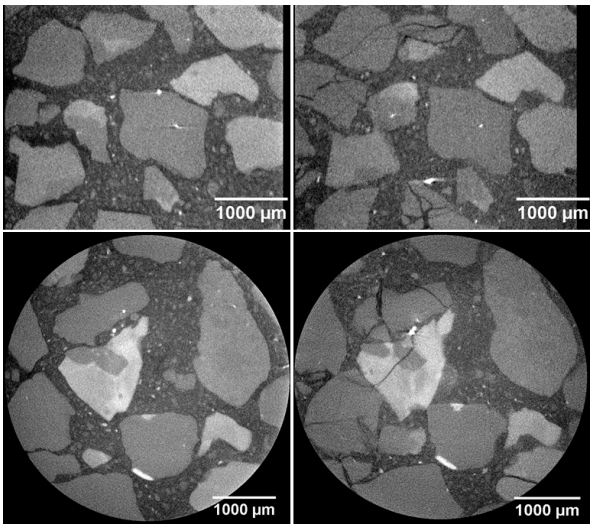

Figure 5: Vertical (top) and horizontal (bottom) slices of μCT images at atmospheric pressure (left) and 13.8 MPa (2000 psi) confining pressure (right). The images clearly show changes in the sample due to pressurization: grain crushing with associated fracturing was observed especially where quartz grains had direct contact points without clay-filled pore space inbetween

RESULTS

Figure 5 shows vertical and horizontal slices through the sample. For comparison, we are showing images at atmospheric pressure prior to compaction and at 13.8 MPa confining pressure. We were able to observe grain damage throughout the entire sample, especially in quartz grains that had direct contact points. Grains that were separated by pore space at atmospheric pressure appear to be crushed against each other at elevated pressure which leads to fracturing.

Figure 6 shows the comparison between an image taken during the first pressure cycle at 13.8 MPa and a subsequent image taken at atmospheric pressure. For some grains we observed that pre-existing fractures extended further and new fractures occured upon decreasing the confining pressure. Some fractures also extended further upon repeated increase of confining pressure pointing to the conclusion that pre-compacted samples experience further change when subjected to increased confining pressure again.

Figure 7 shows images taken during the first pressure cycle at 13.8 MPa, after decreasing the pressure back to atmospheric pressure during the first cycle and after decreasing the pressure back to atmospheric pressure after the second pressure cycle. The bentonite clay in the pore space is compacted upon the application of confining pressure. When the confining pressure

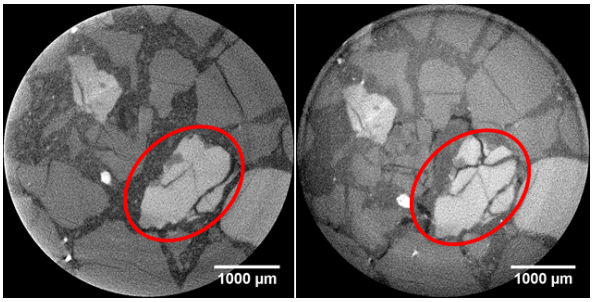

Figure 6: μCT images during first confining pressure increase to 13.8 MPa (2000 psi) (left) and after subsequent decrease to atmospheric pressure. We observed a further progression of existing fractures and opening of new fractures after the confining pressure was decreased between subsequent pressure cycles.

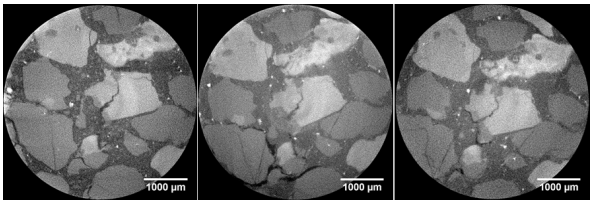

Figure 7: μCT images during first confining pressure increase to 13.8 MPa (2000 psi) (left), after subsequent decrease to atmospheric pressure (middle) and at atmospheric pressure after second confining pressure increase to 13.8 MPa (right). We observed the formation of void spaces especially at quartz grain surfaces (lower half of middle image). As the sample was confined, the clay in the pore spaces was compressed resulting in a volume reduction. The sample expands again after decreasing the confining pressure while the clay stays compacted resulting in voids in the pore space.

is decreased, the clay stays compacted resulting in a decreased volume which leads to the formation of void spaces especially at the grain surfaces of quartz grains. This observed detachment of grains and pore filling materials could potentially lead to decreased stiffness of the sediment. Upon repeated confining pressure cycling these voids seemed to be partially closed again while new ones occurred in oter areas of the sample.

CONCLUSIONS AND FUTURE WORK

We were able to prove the functionality of our pressure and temperature control system and demonstrate that changes in rock samples can be visually observed within the resolution constraints of the Xradia-400 machine. We developed a pressure vessel and ultrasonic transducers suitable for the use in the micro CT machine.

We observed compaction of the sample upon confining pressure increase resulting in grain damage and fracturing of sediment grains. When the confining pressure was decreased some cracks experienced further fracturing. The grain damage appears irreversible. Further fracturing of grains in pre-compacted sediment was observed upon repeated confining pressure cycling.

We are currently working on feed-throughs for fluid lines and electric wiring to use ultrasonic transducers and pressure control in combination. Further we plan to include pore pressure in addition to confining pressure into the system.

The pressure control system in combination with ultrasonic transducers will allow to visually observe pore scale changes in rock samples (such as crack closure, grain damage, porosity reduction, changes in saturation) while simultaneously identifying their influence on ultrasonic velocities. Such pore-scale changes are usually not taken into account by rock physics models and could help to identify why laboratory data diverges from theoretical models. Further, it is possible to compute compressibility from μCT images at different stress states by image correlation (Lenoir et al., 2007; Dautriat et al., 2011; Fusseis et al., 2014).

ACKNOWLEDGEMENTS

This material is based upon work supported by the U.S. Department of Energy (DOE) under Grant Number DEFE0009963. This project is managed and administered by the Colorado School of Mines and funded by DOE/NETL and cost-sharing partners. This report was prepared as an account of work sponsored by an agency of the United States Government. Neither the United States Government nor any agency thereof, nor any of their employees, makes any warranty, express or implied, or assumes any legal liability or responsibility for the accuracy, completeness, or usefulness of any information, apparatus, product, or process disclosed, or represents that its use would not infringe privately owned rights. Reference herein to any specific commercial product, process, or service by trade name, trademark, manufacturer, or otherwise does not necessarily constitute or imply its endorsement, recommendation, or favoring by the United States Government or any agency thereof. The views and opinions of authors expressed herein do not necessarily state or reflect those of the United States Government or any agency thereof.

REFERENCES

Dautriat, J., M. Bornert, N. Gland, A. Dimanov, and J. Raphanel, 2011, Tectonophysics Localized deformation induced by heterogeneities in porous carbonate analysed by multi-scale digital image correlation: Tectonophysics, **503**, 100–116.

Fusseis, F., X. Xiao, C. Schrank, and F. D. Carlo, 2014, Review article A brief guide to synchrotron radiation-based microtomography in (structural) geology and rock mechanics: Journal of Structural Geology, **65**, 1–16.

Lenoir, N., M. Bornert, J. Desrues, P. Besuelle, and G. Viggiani, 2007, Volumetric Digital Image Correlation Applied to X-ray Microtomography Images from Triaxial Compression Tests on Argillaceous Rock: 193–205.

EDITED REFERENCES

Note: This reference list is a copyedited version of the reference list submitted by the author. Reference lists for the 2016 SEG Technical Program Expanded Abstracts have been copyedited so that references provided with the online metadata for each paper will achieve a high degree of linking to cited sources that appear on the Web.

REFERENCES

Dautriat, J., M. Bornert, N. Gland, A. Dimanov, and J. Raphanel, 2011, Localized deformation induced by heterogeneities in porous carbonate analysed by multi-scale digital image correlation: Tectonophysics, **503**, 100–116, http://dx.doi.org/10.1016/j.tecto.2010.09.025.

Fusseis, F., X. Xiao, C. Schrank, and F. de Carlo, 2014, A brief guide to synchrotron radiation-based microtomography in (structural) geology and rock mechanics: Journal of Structural Geology, **65**, 1–16, http://dx.doi.org/10.1016/j.jsg.2014.02.005.

Lenoir, N., M. Bornert, J. Desrues, P. Besuelle, and G. Viggiani, 2007, Volumetric digital image correlation applied to X-ray microtomography images from triaxial compression tests on argillaceous rock: Strain, **43**, 193–205, http://dx.doi.org/10.1111/j.1475-1305.2007.00348.x.